

3D Numerical Investigation on Reservoir System for an Overtopping Wave Energy Converter

Jiyuan Jin*, Zhen Liu**, Keyyong Hong***, † Beom-Soo Hyun

†,* Department of Naval Architecture and Ocean System Engineering, Korea Maritime University, Busan 606-791, Republic of Korea

** College of Engineering, Ocean University of China, Qingdao 266-100, China

*** Maritime and Ocean Engineering Research Institute KORDI, Daejeon 305-343, Republic of Korea

Abstract : *Overtopping Wave Energy Converter (OWEC) is an offshore wave energy converter, which comprises the circular ramp and reservoir. It collects the overtopped waves and converting water pressure head into electric power through the hydro-turbines installed in the vertical duct, which is fixed in the sea bed. The performance of OWEC can be represented by the operating water heads of the device, which depends on the amount of the wave water overtopping into the reservoir. In the present paper, the reservoir with the duct connecting to the sea water are studied in the 3D numerical wave tank, which has been developed based on the computational fluid dynamics software Fluent 6.3. Both the overtopping motion and the discharges of the reservoir are investigated together, and several shape parameters and incident wave conditions are varied to demonstrate their effects on the performance of OWEC.*

Key words : *Wave energy, overtopping, reservoir, Numerical wave tank, operating performance*

1. Introduction

The generation of electric power utilizing clean and renewable ocean resources is one of the most important alternative energy technologies for overcoming shortages in energy resources caused by excessive use of fossil fuels. Among various ocean resources, wave energy is the most abundantly available and applicable in most coastal and offshore areas. Due to the advantages of simple converting technique and producing cost over other types of ocean energy, the wave energy conversion system is feasible to be established for the commercial power production.

Plenty of wave energy absorption devices have been invented, and several of them have been utilized in the electricity generation. Recently, the Oscillating Water Column (OWC) type has been widely employed in the application for the wave energy conversion. The disadvantage of this device is the low wave energy converting efficiency.

Overtopping Wave Energy Converter (OWEC) has the sloping walls and reservoirs to lift waves to the levels above the average surrounding ocean. The released reservoir water is used to drive hydro-turbines or other converting devices. OWEC has several distinct advantages over other types of

wave energy converting devices. It produces a relatively small fluctuation in the derived electricity because it converts wave energy to potential energy in the calm water of the reservoir. Furthermore, OWEC is more feasible economically since it can be combined with other coastal facilities such as breakwaters.

TAPCHAN is a prototype onshore OWEC plant which was installed on a remote Norwegian island in 1985 described by Falnes et al. (1991) and has been functioning ever since. The name is an abbreviation of "tapered channel", which describes the basic idea behind the device. TAPCHAN consists of a reservoir built into a cliff a few meters above the sea level. A tapered channel, which is wide at the mouth and open to the sea, becomes narrower as it penetrates the reservoir. Incoming waves increase in height as they move up the channel, eventually overflowing the lip of the channel and pouring into the reservoir.

Kofoed et al. (2006) proposed a floating wave energy converter of the overtopping type, Wave Dragon. It consists of two patented wave reflectors focusing the wave towards the ramp, linked to the wave reservoir. The wave reflectors have the verified effects of increasing the significant wave height substantially and thereby increasing the energy

* kimkilwon@gmail.com 051)410-4950

** qdsanxian@hotmail.com +86-532-66781125

*** kyhong@moeri.re.kr 042)866-3912

† Corresponding author, bshyun@hhu.ac.kr 051)410-4308

Note) This paper was presented on the subject of "3D Numerical Investigation on Reservoir System for an Overtopping Wave Energy Converter" in Proceedings of the Ninth (2010) ISOPE Pacific/Asia Offshore Mechanics Symposium (Busan, Korea, November 11-17, 2010, pp.137-143)

capture. Waves focused by the reflectors overtop the ramp and fill the reservoir, which is situated at a higher level than the surrounding sea. A study of overtopping flow series on the Wave Dragon prototype was performed by Tedd and Kofoed (2009). A low crested device is designed to maximize flow in a real sea. Their study aimed to fill the gap in the literature on time series of flow overtopping low crested structures. By comparing to a simulated flow the characteristics of the overtopping flow are discussed and the simulation algorithm is tested. The SSG (Sea Slot-cone Generator) is also a wave energy converter of the overtopping type, which was investigated by Margheritini et al. (2009). The structure consists of a number of reservoirs including one on the top of each other above the mean water level in which the water of incoming waves is stored temporary. In each reservoir, expressly designed low head hydro-turbines are converting the potential energy of the stored water into power.

With the development of computer technology and computational dynamics methods, it is feasible to directly solve the Navier-Stokes equations coupled with VOF model for the simulation of many problems, including the wave breaking and overtopping processes, which always include intense air-water interaction.

As mentioned by Lin and Liu (1998), breaking waves in a surf zone by using a VOF based model are calculated to compare with the experimental data. The wave breaking and running up over the structures by using the donor acceptor VOF scheme are simulated by Isobe et al. (2001). Hieu et al. (2004) proposed a numerical two-phase flow model for incompressible viscous fluid utilized in the simulation of wave propagation in the shallow water, including the processes of wave shoaling, breaking, reflection and air movement.

A numerical wave flume is proposed by Reeves et al. (2008) to investigate the discharge characteristics of combined overflow and wave overtopping of impermeable seawalls. The numerical procedure computes solutions to the Reynolds-averaged Navier-Stokes equations and includes the generation of an irregular train of waves, the simulation of wave breaking and interaction with a sloping, impermeable wall. Losada et al. (2008) utilized a two-dimensional numerical model to study the functionality of rubble mound breakwaters. Nam et al. (2008) studied the wave flow over the spiralreef overtopping device using the commercial code Flow 3D to find an optimum device shape with respect to overtopping flow rate.

A 3D numerical wave tank utilizing two-phase VOF model

is established to study the overtopping characteristics and discharge for OWEC device described in the present paper. It has been proved that VOF model can track the free surface and predict the air water interaction which is important for the air water interactions in the overtopping phenomenon. The Reynolds Averaged Navier-Stokes (RANS) equations are employed as the governing equations. The standard $k-\epsilon$ turbulence model is applied to demonstrate the turbulent effects. The Finite Volume Method (FVM), Non-Iterative Time Advancement (NITA) - Pressure Implicit with Splitting of Operators (PISO) algorithm and dynamic mesh technique are used to generate the 2D linear propagating waves. Several incident wave conditions and shape parameters of the reservoir are calculated.

2. Overtopping Wave Energy Converter

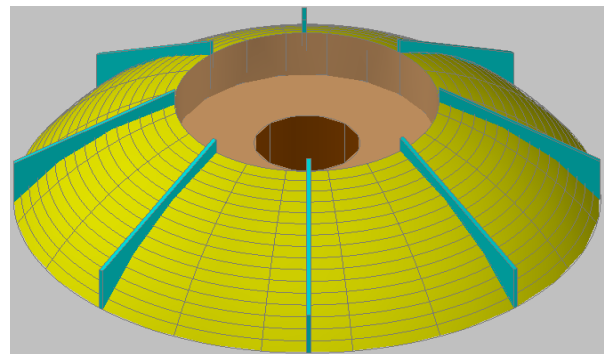


Fig. 1 3D sketch of Roof type Overtopping Wave Energy Converter

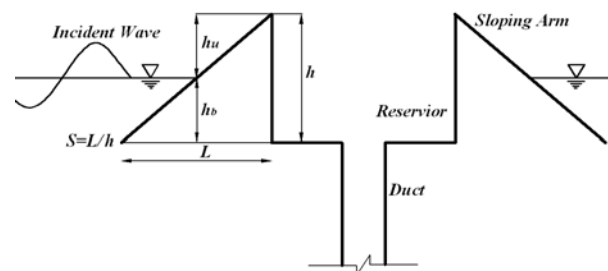


Fig. 2 Schematic of Roof type OWEC

The 3D sketch of the Roof Type Overtopping Wave Energy Converter (OWEC) facility with various types of ramp is illustrated in Fig. 1. The facility consists of a reservoir (Brown component) to store wave water and the round ramp (Yellow components) for the waves to run up from the incident direction. The device is fixed to the sea bottom by the duct installed with the low head

hydro-turbines. In order to guide and instruct the motion of the incident waves and gain more overtopping flow amount, the straight type guide vanes (Blue components) are installed on the ramp.

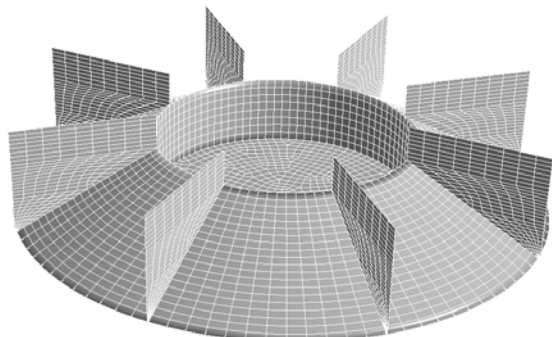


Fig. 3 Surface grid structure of OWEC within guide vanes

The schematic of the OWEC facility can be seen in Fig. 2. As displayed in the figure, L and h represent the projected length and height of the ramp (Sloping Arm) in the horizontal and vertical directions, respectively. The sloping ratio S of the ramp is defined as $S = h : L$. h_u is the hydro head, and h_b is the draft height of the ramp. The water depth is fixed as 20m and the diameter of the reservoir is 15m. The length projected in the oriental direction L varies with respect to the variation of the sloping ratio S and the height projected in the vertical direction h .

3. Mathematical Model

3.1 Governing Equations

In this study, the 3D regular waves have been utilized as the incident waves. The fluids including water and air are incompressible and immiscible. At the interface of two fluids, no phase transit and no-slip between fluids are assumed. The propagating waves are generated by the wave maker plate at the left end, and the opening boundary is set at the other end. The governing equations are the continuity equation and RANS equations for incompressible fluid. The standard $k-\varepsilon$ model, which is widely used in engineering application, is employed to describe the turbulence phenomenon in the water and air dynamic motions.

The tracking of the interface between the air and water phases is accomplished through the Volume of Fluid (VOF) method proposed by Hirt and Nichols (1981). The volume fractions of water and air in the computational cell sum to unity. In addition, the face fluxes through the computational cells are obtained as the geometric reconstruction approach.

The interface between two fluids is calculated using the piecewise-linear scheme (Youngs, 1982), which assumes the linear slope in each cell.

3.2 Numerical Equations

The regular linear wave is applied in the investigation of this paper, and the motion of the piston wave maker is determined from the sinusoid equations. On the opening boundary, the Sommerfeld radiation boundary condition (Sommerfeld, 1949) is used to obtain the relation between the horizontal velocity component and the free surface elevation. The wave absorption can be performed by controlling the motion of the opening boundary within the velocities opposite to the water particles adjacent to the opening boundary on the x -direction.

The motion of the wave generating and absorbing boundaries can be achieved by defining UDF (User-Defined Function) programs. Fluent also provides the layering remeshing method in dynamic mesh model to govern the grid reconstruction adjacent to the moving boundaries. The geometries and meshes are created by the grid generation software Gambit V 2.2, and the grids at the fluid interface have been refined to predict the free surface accurately. The number of grid is about 1.2×10^6 . It means that the gride number for one wave length and wave height are about 100 and 10. The typical surface grid structure of the device within eight guide vanes is shown in Figure 3. The detail description of equations for governing and numerical are presented in Liu et. al. (2008)

The governing equations are solved by using Finite Volume Method (FVM). Second-order upwind discretization is considered for the convection terms. The pressure-velocity coupling is calculated by the NITA (None-Iterative Time Advancement) - PISO (Pressure Implicit with Splitting of Operators) algorithm compatible with VOF model, which requires only one global iteration per time step, and reduces solution time significantly.

In Fluent, the symmetry definition is applied for the wave making and absorbing boundaries. The bottom and chamber structure is set as the wall using no-slip conditions. The pressure outlet is taken account for the upper boundaries of the computational domain adjacent to the air phase.

4. Calculating Validation of OWEC

In order to test the capability of the present 3D numerical wave tank on the simulation of overtopping motion for

OWEC device and operating performance prediction, the roof type OWEC without guide vanes are calculated and validated first.

In the 3D simulation, the numerical wave tank is 250m

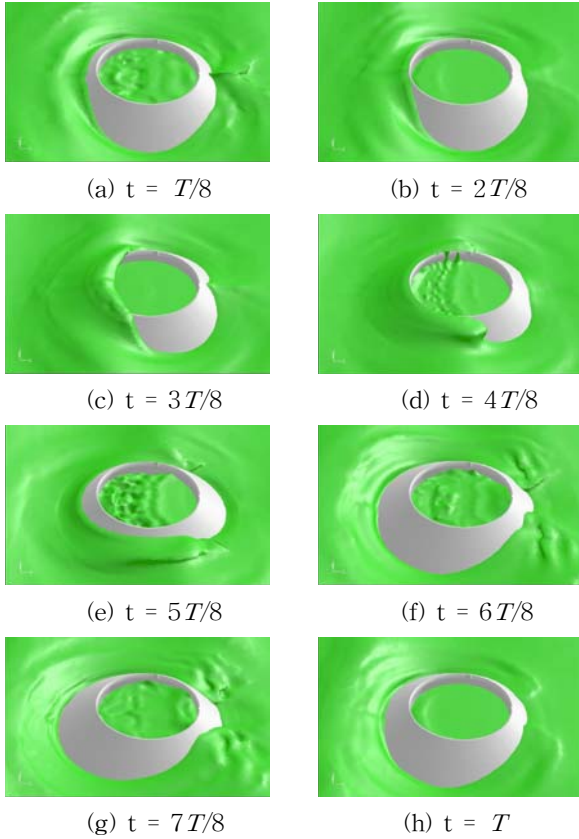


Fig. 4 Snapshots of wave overtopping over OWEC without guide vanes

long, 40m wide and 30m high. A sponge layer for wave damping absorber is set at the opening boundary. The OWEC device is fixed at the position 200m away from the wave maker and 20m away from the side wall.

The typical shape parameters are tested within the common incident wave conditions. The hydro head $h_u=2.0\text{m}$, draft height $h_b=2.0\text{m}$ and the sloping ratio $S=1:1.5$.

The snapshots of overtopping processing for incident wave height $H_0=2.0\text{m}$ within incident wave period $T=5.5\text{s}$ are shown in Figure 4.

It can be seen that there are no evident breakings during the waves run up. The wave water against the front of the device will climb the ramp and only small amount of the climbing water will overtop into the reservoir and other parts at two sides will go on along the ramp. Some of them fall down to the surrounding water and others gather at the end of the device. Generally, most of the climbing waves cannot

finish the overtopping motion because of the round shape of the device.

The overtopping flow rates are monitored and measured by the software automatically. The first five waves are illustrated in Figure 5. It can be seen that the overtopping

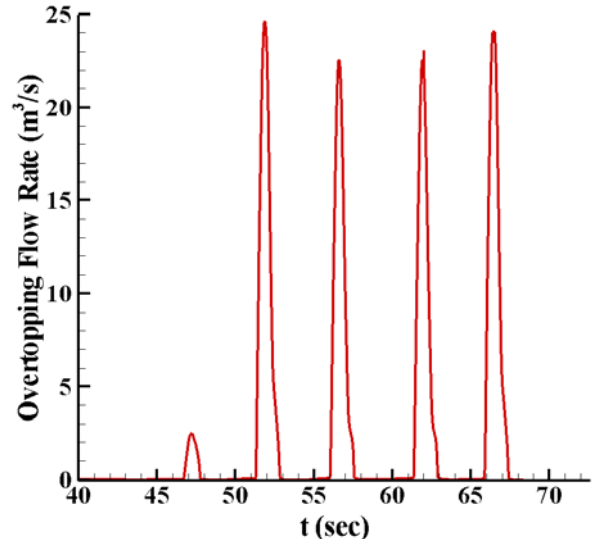


Fig. 5 Overtopping flow rate of OWEC without guide vanes

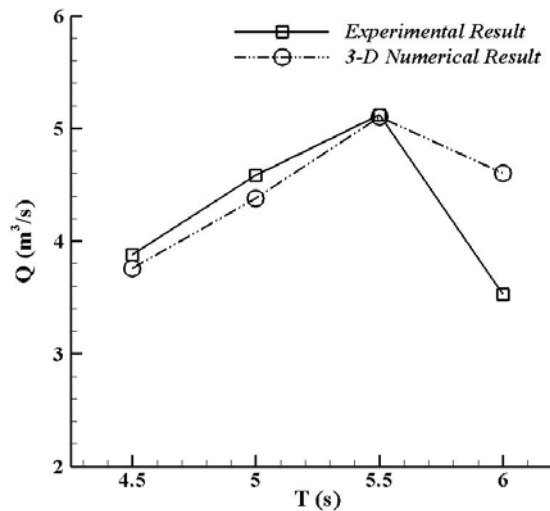


Fig. 6 Comparison of overtopping flow amount of OWEC without guide vanes

flow rate of first wave is smaller than the later ones because of the initial effects of the numerical wave tank. Therefore, the time averaged flow amounts are derived from integrating the flow rates from the second to the sixth waves.

Four incident wave periods are employed in the validation calculation. The 3D numerical predictions are compared with the corresponding experimental data, which is shown in Figure 6. The 3D calculating results agree well with the experimental data for various incident wave periods except

$T=6.0$ s. It is proposed that the difference comes from the model scale effects and basin length limits due to the increasing of wave length within larger wave periods in the experiments. The above disadvantages will not appear in the numerical investigation.

In general, the present 3D numerical model has demonstrated its capability on overtopping phenomena and the operating performance of the roof type OWEC facility and can be utilized in the corresponding analysis.

5. Overtopping Performance of OWEC Device

5.1 Effects of Guide Vane Number

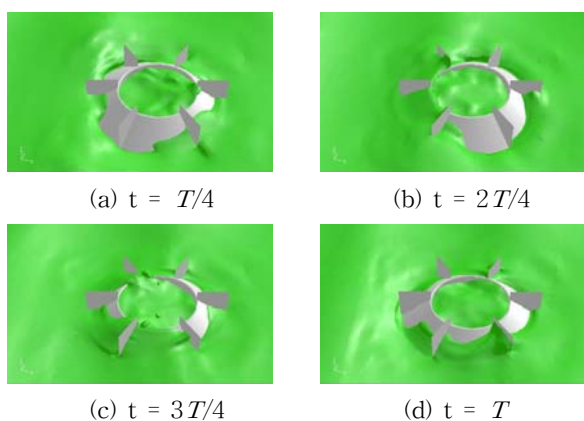


Fig. 7 Snapshots of wave overtopping over OWEC with 6 guide vanes

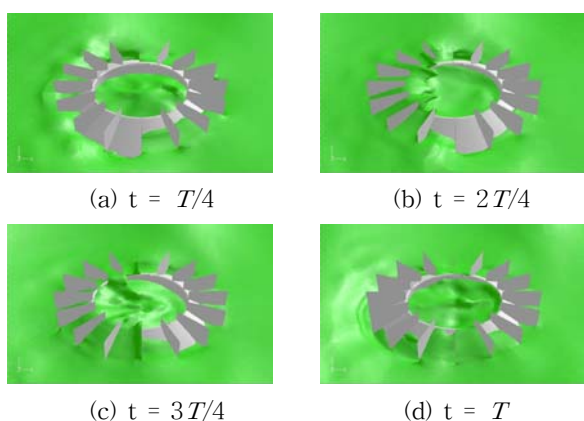


Fig. 8 Snapshots of wave overtopping over OWEC with 12 guide vanes

The straight type guide vane has been tested and proved that it is superior to the spiral type on the improvement of the wave energy converting by the former experiments. Proper number and installation of guide vanes will help the facility to lift and collect some of the wave water

propagating along the side of the facility which originally will fall and go back to the surrounding sea areas. Different number of guide vanes will leave different moving and interaction space for the incident waves, especially the waves

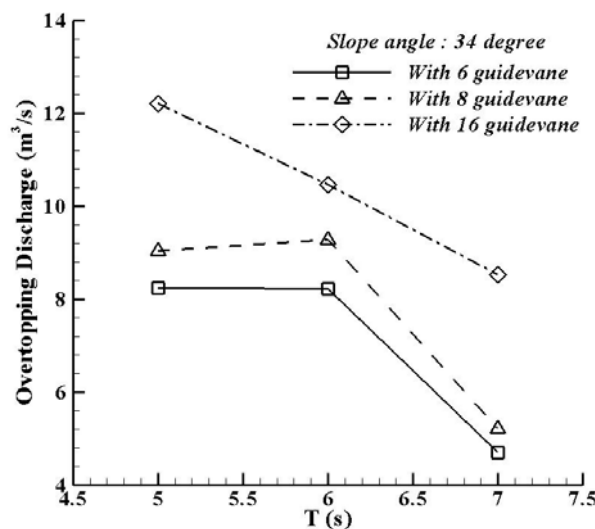


Fig. 9 Effects of guide vane number on the OWEC overtopping discharge

which propagate along the side of the facility.

In order to study the effects of guide vane number, several parameters are selected such as 6, 8 and 16, where $h_u=2.0$ m, $h_b=2.0$ m and $S=1:1.5$. The incident wave conditions are same with the preceding sections.

The snapshots of overtopping processing for 6 and 16 guide vanes within $H_0=2.0$ m, $T=5.0$ s are displayed in Figure 7 and 8. As shown in Fig. 7, the overtopping flow pattern is also influenced by the settling method. However, the gaps between the guide vanes are too large. The guide vanes cannot restrain the wave water propagating along the facility side, which makes the overtopping time averaged discharge is not as high as that of the facility within 8 guide vanes.

On the contrary, the OWEC facility within 16 guide vanes can restrict the flow path and collect most available wave waters along the device side, as shown in Fig. 8. The guide vane also compensate the water lose because of the roof design of the reservoir, which is initially more adaptable to the different incident wave directions.

As mentioned before, the ultimate power output is determined by the hydro head of the water stored in the reservoir. In order to maintain the necessary hydro head, the amount of incident wave water should not be less than that of the released water. It means the time averaged flow amount of the overtopping waves should not be less than the

submerged outflow rate of the duct. Therefore, the time-averaged flow rate should be regarded as one of the most important standards to demonstrate the working performance of the OWEC facility.

The effects of guide vane number on the time averaged overtopping discharge are shown in Fig. 9. The overtopping discharge variation for 6 and 8 guide vanes are almost similar, and there is almost no difference between wave period 5s and 6s for each guide vane number. In general, the performance for 8 guide vanes is a little better than that of 6 guide vanes. The variation for 16 guide vanes shows different characteristics and the overtopping discharges will decrease significantly as the incident wave period increases. Anyway, the energy absorbing efficiency of 16 guide vanes is still higher than that of 6 and 8 guide vanes for each wave period.

Although the operating performance will get better as the number of guide vanes increase, it is necessary to find out the proper number for the guide vane to be utilized on the roof type OWEC.

5.2 Effects of Draft Height

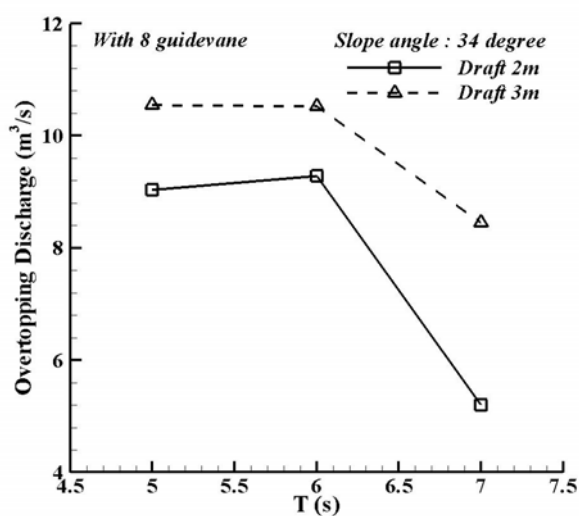


Fig. 10 Effects of draft heights on the OWEC overtopping discharge

In this section, two different draft heights were studied to show the effects of the draft height on the overtopping time averaged discharge of the OWEC facility with 8 guide vanes. The sloping ratio of the ramp and the hydro head are fixed as 1:1.5 (34°) and 2m, respectively. The incident wave height is 2.0m and three wave periods are employed.

Effects of draft heights h_b on the time averaged overtopping discharge are shown in Fig. 10. It can be seen

that the variation characters of the draft heights equal to 2.0m and 3.0m are quite similar. There are no evident differences for the periods between 5.0s and 6.0s, and the overtopping discharge decreases quickly when the period increases to 7.0s.

The overtopping discharges for $h_b=3.0\text{m}$ at every wave period are significantly higher than that of $h_b=2.0\text{m}$. The above results illustrate that the deeper draft will help the facility to collect more energy for the wave water to climb up and overtop. On the other hand, it was found that the deeper draft will induce more impacting wave force because collecting more energy means to face more energy. The huge impacting wave force may cause the unpredictable damages to the facilities.

Therefore, we cannot just concentrate on the improvement of the operating efficiency and ignore the safety of the converter. It is necessary to carry out more research to consider the performance and safety at the same time to select the proper draft height.

6. Conclusion

In the present paper, a 3D numerical wave tank based on two-phase VOF model is extended from 2D case and established to be applied in the numerical investigation on the 3D roof type overtopping wave energy converter.

The 3D numerical wave tank has been validated by the corresponding experimental data, typical sea wall overtopping problem and the roof type OWEC without guide vanes have been employed. All the calculating results illustrate that the present 3D numerical wave tank is not only superior to the corresponding 2D one, but also capable to be employed for the analysis of complicated free surface analysis, such as the overtopping phenomena.

Several key shape parameters are studied to help improving the design and optimization of the OWEC with guide vanes. Although deeper draft can contribute the wave energy absorbing and converting, it will also induce the higher wave force impacts which maybe is fatal or an underlying safety problem. Therefore, it is necessary to analyze the operating performance and the wave force together to gain the proper draft values.

In the present paper, the increasing of guide vane number will increase the overtopping time averaged discharges significantly. It is unknown that if the number of the guide vanes keeps increasing, the overtopping discharges will increase correspondingly and if there is an upper limit or the

restricted domain.

Anyway, it still needs more numerical studies collaborating with experiments to keep discovering the operating mechanism and improving the running efficiency for the ultimate design, optimization and practical utilization of the Roof Type Overtopping Wave Energy Converter.

Acknowledgements

This research is financially supported by Korea Ocean Research & Development Institute (Development of Wave Energy Utilization System), and MKE of Korea through New & Renewable Energy R&D Program (No.20093021070010 and No.20093020070020). All the support is gratefully acknowledged.

References

- [1] Falnes, L. and Loveseth, J. (1991), "Ocean Wave Energy", *Energy Policy*, Vol. 19, No. 8, pp. 768~775.
- [2] Hieu, P.D., Katsutoshi, T. and Ca, V.T. (2004), "Numerical Simulation of Breaking Waves using a Two-phase Flow Model", *Applied Mathematical Modeling*, Vol. 28, No. 11, pp. 983~1005.
- [3] Hirt, C.W. and Nichols, B.D. (1981), "Volume of Fluid (VOF) Method for the Dynamics of Free Boundaries", *J Comp Phys*, Vol. 39, pp. 201~225.
- [4] Isobe, M. (2001), "A VOF-based Numerical Model for Wave Transformation in Shallow Water", In *Proc Int. Workshop on ADMS21, PHRI*, pp. 200~204.
- [5] Kofoed, J.P., Frigaard, P., Madsen, E.F. and Sorensen, H.C. (2006), "Prototype Testing of the Wave Energy Converter Wave Dragon", *Renewable Energy*, Vol. 31, No. 2, pp 181~189.
- [6] Lin, P. and Liu, PL-F (1998), "A Numerical Study of Breaking Waves in the Surf Zone", *J Fluid Mech*, Vol. 359, pp. 239~264.
- [7] Liu, Z., Hyun B.S. and Jin J.Y. (2008), "Numerical Prediction for Overtopping Performance of OWEC", *Journal of the Korean Society for Marine Environmental Engineering*, Vol. 11, No. 1, pp. 35~41.
- [8] Losada, I.J., Lara, Javier L., Guanche, R. and Gonzalez-Ondina J.M. (2008), "Numerical analysis of wave overtopping of rubble mound breakwaters", *Coastal Engineering*, Vol. 55, pp. 47~62.
- [9] Margheritini, L., Vicinanza, D. and Frigaard, P. (2009), "SSG wave energy converter: Design, reliability and hydraulic performance of an innovative overtopping device", *Renewable Energy*, Vol. 34, pp. 1371~1380.
- [10] Nam B.W., Shin S.H., Hong K.Y. and Hong S.W. (2008), "Numerical simulation of the wave flow over the spiral-reef overtopping device", *Proceedings of the Eighth (2008) ISOPE Pacific/Asia Offshore Mechanics Symposium, Bangkok, Thailand*, Vol. 1, pp. 262~267.
- [11] Reeve, D.E., Soliman, A. and Lin P.Z. (2008), "Numerical study of combined overflow and wave overtopping over a smooth impermeable seawall", *Coastal Engineering*, Vol. 55, pp. 155~166.
- [12] Tedd, James and Kofoed, J.P. (2009), "Measurements of overtopping flow time series on the Wave Dragon, wave energy converter", *Renewable Energy*, Vol. 34, pp. 711~717.
- [13] Sommerfeld, A. (1949), "Partial Differential Equation in Physics", Academic Press, New York.
- [14] Youngs, D.L. (1982), "Time-dependent Multi-material Flow with Large Fluid Distortion", *Num Meth Fluid Dynamics*, Academic Press, New York.

Received 13 February 2012

Revised 28 March 2012

Accepted 28 March 2012